[CANCER RESEARCH 64, 1621–1631, March 1, 2004]

Microenvironmental Regulation of Proliferation in Multicellular Spheroids Is Mediated through Differential Expression of Cyclin-Dependent Kinase Inhibitors

Karen E. A. LaRue, Mona Khalil, and James P. Freyer

Bioscience Division, Los Alamos National Laboratory, Los Alamos, New Mexico

ABSTRACT

Multicellular spheroids composed of transformed cells are known to mimic the growth characteristics of tumors and to develop gradients in proliferation with increasing size. This progressive accumulation of quiescent cells is presumably an active process that occurs in response to the microenvironmental stresses that develop within the three-dimensional structure, and, yet, little is known regarding either the signals that induce the cell cycle arrest or the molecular basis for the halt in proliferation. We have previously reported that regulation of cyclin-dependent kinase (CDK) inhibitors (CKIs) differs in monolayer *versus* spheroid cell culture. In this study, we have examined the expression of three CKIs in EMT6 mouse mammary carcinoma and MEL28 human melanoma spheroids, as a function both of spheroid size and of location within the spheroid. We report that expression of the CKIs $p18^{INK4c}$, $p21^{waf1/cip1}$, and $p27^{Kip1}$ all increase as the spheroid grows and develops a quiescent cell fraction. However, by examining protein expression in discrete regions of the spheroid, we have found that only $p18^{INK4c}$ and $p27^{Kip1}$ expression positively correlate with growth arrest, whereas $p21^{waf1/cip1}$ is expressed predominantly in proliferating cells. Further analysis indicated that, in the quiescent cells, $p18^{INK4c}$ is found in increasing association with CDK6, whereas $p27^{Kip1}$ associates predominantly with CDK2. In MEL28 cells, CDK2 activity is completely abrogated in the inner regions of the spheroid, whereas in EMT6 cells, CDK2 activity decreases in accordance with a decrease in expression. We also observed a decrease in all cell cycle regulatory proteins in the innermost spheroid fraction, including CDKs, CKIs, and cyclins. Induction of CKIs from separate families, as well as their association with distinct target CDKs, suggests that there may be multiple checkpoints activated to ensure cell cycle arrest in non-growth-conducive environments. Furthermore, because very similar observations were made in both a human melanoma cell line and a mouse mammary carcinoma cell line, our results indicate that these checkpoints, as well as the signal transduction pathways that activate them, are highly conserved.

INTRODUCTION

The multicellular spheroid has long been accepted as an *in vitro* model of solid tumors (1–3). As is observed within tumors, continued spheroid growth leads to the progressive accumulation of a quiescent subpopulation of cells in the aggregate center. This quiescent cellular subpopulation is analogous to those regions within tumors in which the vasculature is inadequate or occluded, resulting in a hypoxic mass of nonproliferating cells that are resistant to many current therapies (4, 5). Cell cycle arrest within spheroids and tumors has been attributed to microenvironmental stresses, such as deprivation of oxygen, growth factors and/or nutrients, or the production of inhibitory factors from quiescent or necrotic cells (6–8). However, there is no direct evidence to support any mechanisms or causative agents, and very little is known about the molecular regulation of cell cycle progression in the inner regions of spheroids, or in the non proliferating regions of tumors.

Cell cycle progression is often regulated by the expression and activity of cyclins, cyclin dependent kinases (CDKs), CDK activators, and CDK inhibitors (CKIs; Refs. 9–11). The CKIs consist of two families that are grouped according to their protein structure (12). The members of the INK4 (inhibitor of CDK4) family of CKIs, $p16^{INK4a}$, $p15^{INK4b}$, $p18^{INK4c}$, and $p19^{INK4d}$, form binary complexes with CDKs 4 and/or 6 (13, 14). This association obstructs CDK/cyclin interaction, and the subsequent phosphorylation and inactivation of the retinoblastoma (Rb) protein and thereby inhibits the gene expression required for G_1- to S-phase progression (15). The INK4 CKI family has been implicated in cell differentiation and senescence (16–18) and has received a lot of attention because of the observation that some members are often mutated or deleted in human cancers (19, 20). The other CKI family includes $p21^{waf1/cip1}$, $p27^{Kip1}$, and $p57^{Kip2}$. These proteins have been detected, at least *in vitro*, in complexes with cdc2 (CDK1), CDK2, CDK4, and CDK6, and cyclins A, B, D, and E and, thus, could potentially act as universal cell cycle inhibitors. However, *in vivo*, overexpression of $p21^{waf1/cip1}$ and $p27^{Kip1}$ leads to G_1 arrest (21, 22), suggesting that, despite their broad *in vitro* specificity, this CKI family is also primarily involved in the regulation of G_1-phase progression. It is important to note that this second family of CKIs are often found in proliferating cells, in which they are thought to act as adaptor proteins that assemble and program kinase complexes for specific functions (23). However, protein expression increases in response to a variety of stresses, and the alteration in the ratio of CKI:cyclin/CDK determines the promoting or inhibitory activity of these molecules (24).

We have recently demonstrated that the signals that regulate CKI expression differ in monolayer *versus* multicellular spheroid culture (25). In fact, it is becoming increasingly clear that cells in spheroid culture (26, 27), and even plateau-phase monolayer culture (28), respond differently to a variety of growth-perturbing signals and drugs than do exponentially growing monolayer cultures. For these reasons, we have chosen the model that most closely mimics growth regulation in solid tumors, the multicellular spheroid, to begin to elucidate the molecular mechanisms, as well as the physiological signals, that induce quiescence in tumors.

In this study, we have determined that cell cycle arrest in mouse mammary carcinoma EMT6 spheroids and human melanoma MEL28 spheroids is an active process regulated by the induction of specific CKIs. We demonstrate that as the spheroid grows from a small aggregate containing only proliferating cells to one containing predominantly G_1-phase-arrested cells, the overall levels of $p18^{INK4c}$, $p21^{waf1/cip1}$, and $p27^{Kip1}$ increase. However, by examining the levels of these proteins in specific regions of the spheroid, we show that only $p18^{INK4c}$ and $p27^{Kip1}$ expression correlates with growth arrest, whereas $p21^{waf1/cip1}$ decreases as cells enter a quiescent state. These results suggest that the expression of these three proteins is regulated by different microenvironmental signals. We also found that $p18^{INK4c}$ and $p27^{Kip1}$ associate with, and inactivate, different CDK/CKI complexes in quiescent cells that come from spheroids, suggesting that

Received 10/1/02; revised 10/13/03; accepted 12/30/03.

Grant support: Supported by NIH Grants ES07845, CA71898, and CA80316; by the Department of Energy; and by the Laboratory Directed Research and Development program of the Los Alamos National Laboratory.

The costs of publication of this article were defrayed in part by the payment of page charges. This article must therefore be hereby marked *advertisement* in accordance with 18 U.S.C. Section 1734 solely to indicate this fact.

Requests for reprints: James P. Freyer, Bioscience Division, Mail Stop E535, Los Alamos National Laboratory, Los Alamos, NM 87545. E-mail: freyer@lanl.gov.

there are multiple checkpoints activated by the spheroid microenvironment to ensure cell cycle arrest under non-growth-conducive conditions. Finally, we also show that the most microenvironmentally stressed cells have decreased levels of all of the cell cycle regulatory proteins measured, including CDKs, CKIs, and cyclins.

MATERIALS AND METHODS

Cell Lines and Monolayer Culture. EMT6 mouse mammary carcinoma cells (29), obtained from Dr. Robert Sutherland (University of Rochester, Rochester, NY), and MEL28 human melanoma cells (30), obtained from the American Type Culture Collection (HTB-72), were cultured in α-MEM, supplemented with 10% fortified bovine calf serum (Cosmic Calf Serum; Hyclone Laboratories) and antibiotics (50 μg/ml streptomycin and 50 units/ml penicillin; Life Technologies, Inc.), hereafter referred to as complete medium. Monolayer cultures were maintained in treated polystyrene culture flasks or dishes in a 37°C incubator containing a humidified atmosphere of 5% CO_2 and 95% air. Cells were detached from dishes by incubation in 0.25% trypsin (Difco) in Puck's saline A containing 1 mM EDTA and 25 mM HEPES (pH 7.4). After the addition of complete medium, cell suspensions were passed twice through an 18-gauge needle to disrupt cell clumps.

Spheroid Culture and Assay. Spheroids were initiated by inoculating 1×10^5 exponentially growing EMT6 or MEL28 cells into 100-mm dishes containing 15 ml of complete medium on top of an underlayer of 0.5% agarose (Sigma Chemicals) in complete medium. After 1 day, the spheroids were removed by decanting the medium, were pelleted by centrifugation ($100 \times g$, 5 min), and were resuspended in complete medium. Most of this spheroid suspension was placed into spinner culture. Aliquots of the spheroid suspension were diluted with PBS (Life Technologies, Inc.), and the number of spheroids/ml was determined by counting five replicate samples. A sample of the spheroids was sized with a microscope-based image processing system interfaced to a personal computer (Macintosh) using a video capture board (Scion) and the NIH Image analysis software. The major and minor axes of 25 separate spheroids were determined, and a geometric mean diameter was calculated. Each diameter measurement was calibrated against an image of a fixed spheroid of known diameter measured using the same microscope settings. An aliquot of the spheroid suspension was pelleted by centrifugation, resuspended in the same trypsin solution used for monolayer cultures, and incubated at 37°C for 10 min. After the trypsin exposure, cell suspensions from spheroids were handled as described above for suspensions of cells from monolayers. The mean cell number per spheroid was estimated by dividing the total number of cells recovered by the number of spheroids in the aliquot. One-half of the spheroids were removed from the spinner flask each day and were used for the assay of spheroid number, diameter, cells per spheroid, and protein analysis. The remaining spheroids were replaced in spinner culture with fresh complete medium.

Large diameter spheroids were obtained by spinner culture of aggregates, essentially as described in detail earlier (31, 32). After 4–5 days of culture in agarose-coated dishes, spheroids were size selected by sedimentation and were transferred to 500 ml of complete medium in a spinner flask (Belco), equilibrated with 500 ml of 5% CO_2 in 95% air, and spun at 200 rpm in a 37°C water bath. The medium and gas mixture were replaced daily thereafter, and aliquots of spheroids were removed daily to keep the total number of cells in the flask below 10^8 (2×10^5 cells/ml).

Spheroid Selective Dissociation. Large spheroids were dissociated into subpopulations of cells from different locations in the spheroid essentially as described previously (33) but using a specially designed suspension chamber described in detail elsewhere.[1] Briefly, 500 spheroids were size-selected to yield a population with a mean diameter between 1200 and 1300 μm, with the coefficient of variation of the diameter for any given spheroid population <5%. The spheroids were then placed in a cylindrical chamber and perfused such that the aggregates remained in the bottom of the chamber, and the perfusate flowed out of the chamber through a 75-μm nylon mesh. After washing the spheroids with PBS as a perfusate, they were switched to a dissociation solution containing 0.125% trypsin (Life Technologies, Inc.) in a phosphate buffer containing 1 mM EDTA and 25 mM HEPES to maintain the pH at 7.4. Cells dissociated from the spheroids flowed out of the chamber and were collected into stirred tubes containing complete medium on ice, and the remaining aggregates remained in the chamber. Careful control of the perfusion rate and the number of spheroids in the chamber resulted in the dissociation of cells from the outer spheroid surface, so that sequential collections of dissociated samples resulted in cell suspensions from different locations in the spheroid viable rim.[1] The dissociation rate was 2–3% of the total spheroid cell content per minute, resulting in a total dissociation time of 30–36 min. Cell suspensions were stored on ice until dissociation was complete. Locations of the dissociated fractions were calculated from the cell counts and measurements of the viable cell rim, as described in detail previously (33).[1] On the basis of variation in cell counts and histological observations (33),[1] the location of the cell fractions is estimated to vary by less than 10 μm.

Cell Counting and Volume Analysis. Three counts of each cell suspension were determined with an electronic particle counter (Coulter Electronics) interfaced with a pulse-height analyzer. Counts were taken only on that region of the cell volume distribution that excluded small-volume acellular debris. A cell volume distribution containing $>10^4$ cell measurements was saved for each sample and were analyzed to estimate the mean cell volume of the population. Volumes were calibrated by measurement of polystyrene spheres 7–21 μm in diameter.

Flow Cytometric DNA Content Analysis. An aliquot containing 10^6 cells of each cell suspension was pelleted by centrifugation ($1000 \times g$, 10 min), resuspended in PBS, and fixed in 70% ethanol. Fixed cell samples were washed once with PBS and then were resuspended in PBS containing either 0.5 μg/ml Hoechst 33342 or 50 μg/ml propidium iodide (Sigma) with 100 μg/ml RNase Type I (Sigma). Stained samples were analyzed on a flow cytometer (Becton Dickinson FACS Calibur) to collect DNA content histograms containing $>10^4$ cells. Histograms were analyzed for cell cycle phase distribution with MacCycle (Phoenix Flow Systems) using correction for background debris and aggregates.

Flow Cytometric Proliferation Analysis. Spheroids were exposed to a 30-min pulse label with 30 μg/ml bromodeoxyuridine (BrdUrd), were quickly washed three times in cold (2°C) complete medium, and then were dissociated as described above. The cell suspensions were then fixed in 70% ethanol and kept at 2°C until flow analysis. Fixed cells were washed with balanced salt solution and then were stained with a combination of 25 μg/ml Hoechst 33342 and 10 μg/ml mithramycin. Both of these dyes fluorescently label DNA specifically, but the Hoechst fluorescence is reduced by the incorporation of BrdUrd into the DNA, whereas the mithramycin fluorescence is largely unaffected. Collection of both fluorescent signals in a list-mode fashion for each cell allows the derivation of a difference signal, which can be analyzed to determine the fraction of BrdUrd-incorporating cells in each cell cycle phase (34). Analysis of cells from an exponentially growing monolayer showed that only 1–2% of the S-phase cells did not register as BrdUrd positive.

Western Analysis. Whole cell extracts were prepared by lysing the cells in four cell pellet volumes of radioimmunoprecipitation assay (RIPA) buffer [0.15 M NaCl, 1% sodium deoxycholate, 0.1% SDS, 1% Triton 100, and 50 mM Tris-HCl (pH 7.4)] for 30 min at 4°C. Samples involving large spheroids were further treated by triturating through a 22-gauge needle. The lysates were clarified by centrifugation at $13{,}200 \times g$, and protein concentration was determined by the D_C Protein assay (Bio-Rad). Fifty μg of protein per lane were diluted in sample buffer [10% 2-mercaptoethanol, 2% SDS, 30% glycerol, 0.025% bromphenol blue, 50 mM Tris-HCl (pH 6.8)], fractionated on a 12% gel by SDS-PAGE, and then transferred to nitrocellulose membranes. Protein expression was detected by enhanced chemiluminescence (DuPont New England Nuclear) with rabbit polyclonal antibodies purchased from Calbiochem and Santa Cruz Biotechnology. $p27^{Kip1}$ was detected using (Santa Cruz) sc-528, a rabbit IgG raised against the COOH-terminal 19-amino-acid sequence of human p27. $p18^{INK4c}$ was detected using sc-1208, a rabbit IgG raised against amino acids 1–168 representing full-length $p18^{INK4c}$ of mouse origin. CDK2 was detected using sc-163, a rabbit IgG raised against an amino acid sequence mapping to the COOH terminus of CDK2 of human origin. CDK4 was detected using sc-601, a rabbit IgG raised against an amino acid sequence mapping to the COOH terminus of CDK4 of human origin. CDK6 was detected using sc-177, a rabbit IgG raised against an amino acid sequence mapping to the COOH terminus of CDK of human origin. Cyclin A was detected using sc-751, a rabbit IgG raised against amino acids 1–432 repre-

[1] J. P. Freyer, J. H. Coulter, M. Kahlil, and K. E. A. LaRue. An automated perfusion system for the selective dissociation of multicellular spheroids, submitted for publication.

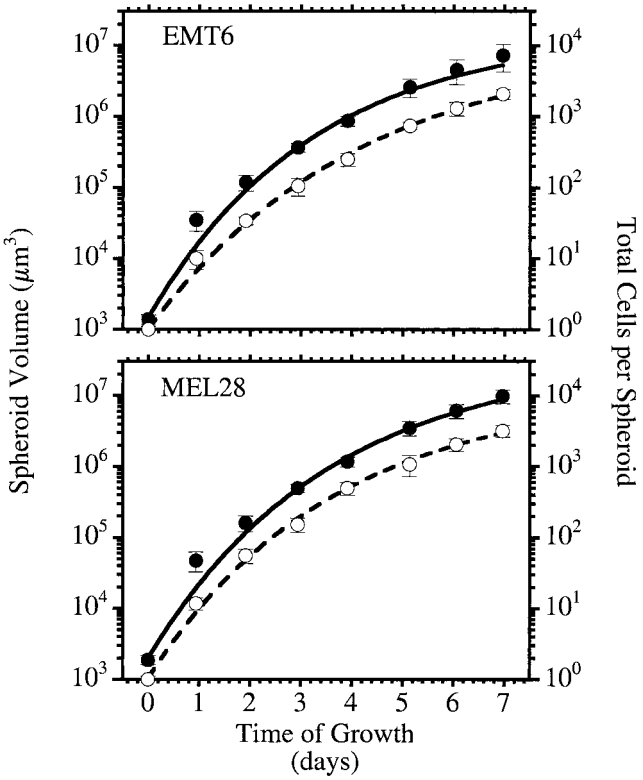

Fig. 1. Growth of EMT6 (*top panel*) and MEL28 (*bottom panel*) spheroids in terms of mean spheroid volume (●, solid line) and total number of cells per spheroid (○, dashed line) as a function of time in culture. *Data points*, means ± SDs of three replicate experiments; *lines*, nonlinear least-squares best fits to the Gompertz equation ($r > 0.98$).

senting full-length cyclin A of human origin. Cyclin D1 was detected using sc-246, a mouse IgG1. Cyclin E was detected using sc-481, a rabbit IgG raised against an amino acid sequence mapping to the COOH terminus of Cyclin E of rat origin. $p21^{waf1/cip1}$ was detected using anti-waf-1 (Ab5) from Calbiochem. The molecular weight of bands was determined using a broad-range protein ladder standard (Bio-Rad). Digitized images of the gels were quantitated using the NIH Image program to calculate the mean intensity and area of each band. All of the quantitations are expressed relative to a single band in each gel, either the initial time in the time course measurements (Fig. 4) or the outermost cell fraction (Fig. 7).

Immunohistochemistry of Spheroid Sections. For immunohistochemical analysis of CKI expression, several spheroids were removed from a spinner flask and placed immediately into ice-cold PBS. Individual spheroids were removed, mixed with frozen tissue-embedding medium (HistoPrep; Fisher Scientific), and immediately frozen on a block of brass cooled in liquid nitrogen. The maximum time elapsed between any spheroid being in the culture vessel and being frozen was 5 min. Frozen spheroids were cut into 5-μm-thick sections using a cryotome and prepared for immunohistochemistry analysis using standard techniques as described in detail elsewhere (35). Sections were processed for immunohistochemistry, as described previously for frozen tumor sections (35) using the same antibodies as for the Western analysis followed by a fluorescein–labeled secondary antibody. Sections were counterstained with 4′,6-diamidino-2-phenylindole (DAPI) to visualize the nuclei, and false-color digital images of the two fluorochromes were created using standard image processing techniques (35).

Immunoprecipitation and Kinase Activity Analysis. Whole cell extracts were prepared by lysing the cells in four cell pellet volumes of lysis buffer [50 mM Tris-HCl (pH 7.9), 150 mM NaCl, 20 mM EDTA, 0.5% NP40] for 30 min at 4°C. The lysates were clarified by centrifugation at 13,200 × *g*, diluted to 10^7 cells/ml in lysis buffer and frozen at −70°C. For coimmunoprecipitation analysis, 10^6 cell equivalents were diluted in 1 ml of lysis buffer, followed by the addition of 20 μg of primary antibody-agarose conjugate (Santa Cruz Biotechnology), or 1 μg of primary antibody plus 15 μl of Protein G-plus agarose (Santa Cruz Biotechnology). The lysates were incubated with rocking for 16 h at 4°C; the beads were washed three times in cold PBS, resuspended in sample buffer (as above), and heat denatured at 95°C for 10 min. Samples equivalent to 2.5×10^5 cells per lane were fractionated on a 12% gel by SDS-PAGE, and protein expression was detected as described above. To assay cyclin-dependent kinase activity, immunoprecipitated kinase complexes were suspended in kinase buffer (for CDK6: 50 mM HEPES, 5 mM $MnCl_2$, 10 mM $MgCl_2$, and 1 mM DTT; for CDK2: 50 mM Tris-HCl, 10 mM $MgCl_2$, and 1 mM DTT), and the reaction was initiated by the addition of ATP, [γ-^{32}P]ATP (NEN BLU502Z, 6000 Ci (222 TBq)/mmol), and substrate. The substrates were purified histone H1 (Boehringer Mannheim) for assessment of CDK2 activity and a GST-tagged COOH-terminal fragment of the retinoblastoma protein (Santa Cruz Biotechnology) for assessment of CDK6 activity. The reaction proceeded for 15–30 min at 30°C and was stopped by the addition of SDS sample buffer. The total reaction mix was applied to a gel, the proteins were fractionated, and bands were visualized by autoradiography.

RESULTS

Cell Cycle Distribution during Spheroid Growth. It has been previously reported that EMT6 cells cultured as spheroids are progressively accumulated in a quiescent state with continued growth (31, 32). To examine the kinetics of this arrest, and to elucidate at which phase of the cell cycle it was occurring, we cultured EMT6 and MEL28 cells as spheroids for 7–8 days. At 24-h intervals, the multicellular aggregates were collected, sized, and dissociated by trypsinization; the cell yield was counted, and the cells were fixed and stained for DNA content analysis. In both cell lines, spheroid growth was well described by a Gompertz equation, indicating initial exponential growth with a progressively decreasing growth rate (Fig. 1). As shown in Fig. 2, there was a continuous increase in the G_1-phase fraction over the entire growth period, with a corresponding decrease

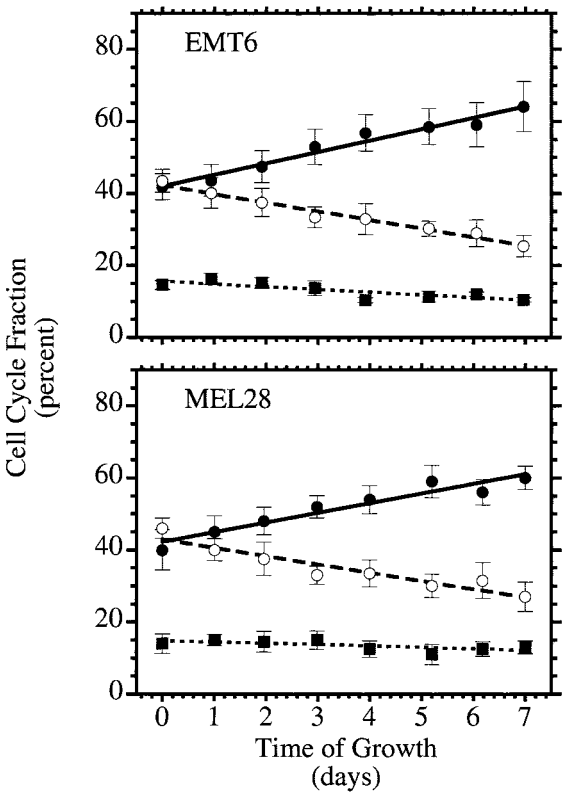

Fig. 2. Fraction of the cell population with G_1- (●, solid line), S- (○, dashed line) or G_2-phase (■, dotted line) DNA content as a function of time of growth of EMT6 (*top*) and MEL28 (*bottom*) spheroids, with *data at time zero* representing cells from exponentially growing monolayer populations. *Data points*, means ± SDs ($n = 3$); *lines*, least-squares best fits to a linear equation ($r > 0.95$).

in the S-phase fraction and little change in the G_2-phase fraction. However, the spheroid size and cell number continued to increase (Fig. 1), indicating that there was a mixture of proliferating and quiescent cells in the spheroids (32).

G_1-Phase Regulatory Protein Expression during Spheroid Growth. To determine whether the accumulation of G_1-phase cells observed during EMT6 and MEL28 spheroid growth was due to changes in the expression of proteins known to be involved in G_1-phase progression, Western analyses were performed on whole-cell lysates obtained from spheroids cultured for 0 (exponentially growing monolayer cells) to 7 days as nonadherent, multicellular aggregates (Figs. 3 and 4). We found that in both cell types, the expression of $p21^{waf1/cip1}$ was up-regulated by 24 h of culture on the agarose dishes. In EMT6 cells, the level of $p21^{waf1/cip1}$ doubled over the first 2 days in spheroid culture and then remained constant. In MEL28 cells, the amount of $p21^{waf1/cip1}$ doubled in the first 3 days of spheroid culture and then declined to a level approximately one-half of that in the exponentially growing cells. $p18^{INK4c}$ and $p27^{Kip1}$ were also rapidly induced and continued to increase to a level that was three or four times that found in exponentially growing cells. The increase in $p18^{INK4c}$ and $p27^{Kip1}$ was more rapid in the EMT6 cells than in the MEL28 cells. There were no significant changes in the expression of either G_1-phase cyclins (D1 or A) or CDKs (2, 4, or 6) in this initial growth period (data not shown).

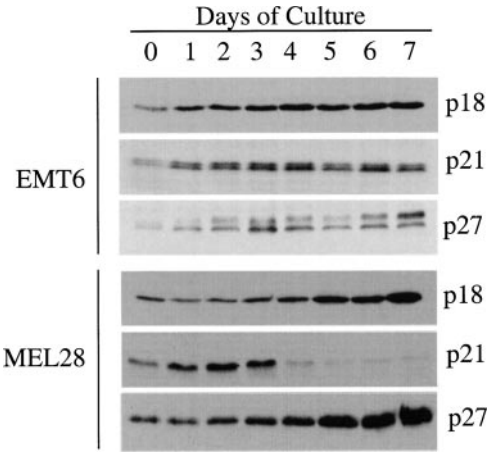

Fig. 3. Western analysis of cyclin-dependent kinase inhibitor (CKI) expression in EMT6 (*top panel*) and MEL28 (*bottom panel*) spheroids as a function of time in culture. *Data*, representative of results from independent experiments and correspond to the eight time points (*days 0–7*) shown in Figs. 1 and 2.

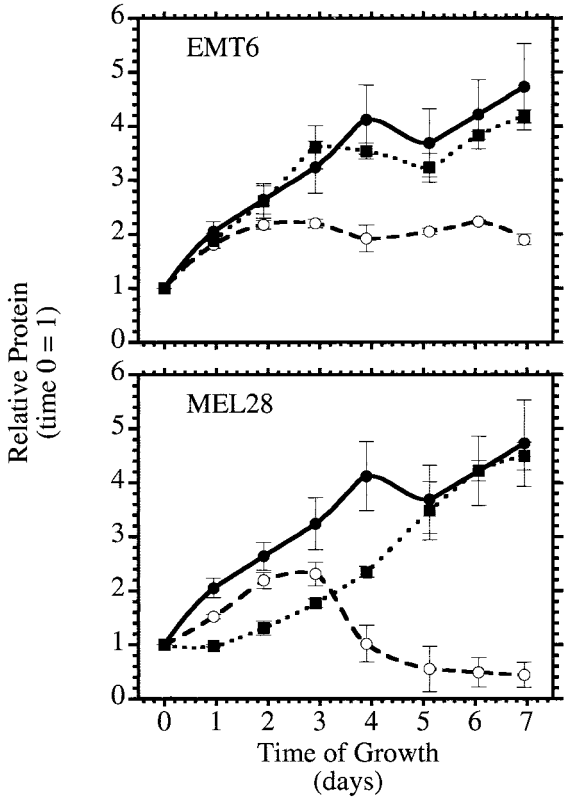

Fig. 4. Amounts of p18 (●, solid line), p21 (○, dashed line), and p27 (■, dotted line) in EMT6 (*top panel*) and MEL28 (*bottom panel*) spheroids as a function of time in culture, expressed relative to the amount of protein detected at time zero (initiation of spheroid culture) on each separate gel. Values are means ± SEs of the mean for three (*EMT6*) or two (*MEL28*) separate experiments; *lines*, interpolations to the data.

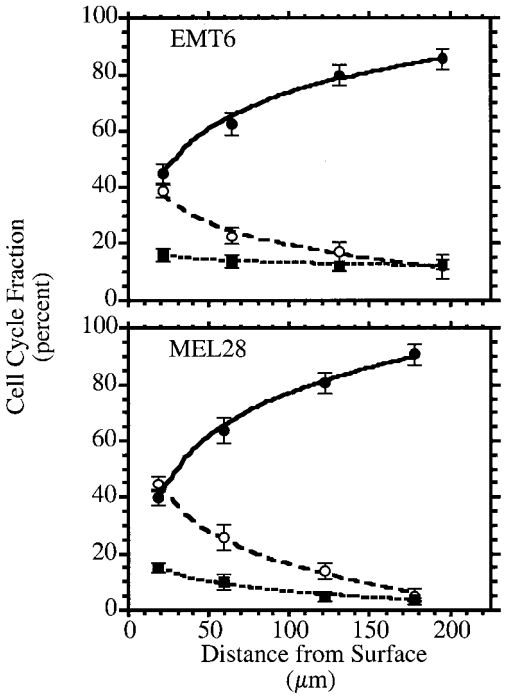

Fig. 5. Fraction of the cell population with G_1- (●, solid line), S- (○, dashed line), or G_2-phase (■, dotted line) DNA content as a function of location within EMT6 (*top panel*) and MEL28 (*bottom panel*) spheroids of ~1200 μm in diameter. Data points and *error bars* are as described in Fig. 2 ($n = 3$); *lines*, least-squares best fits to a logarithmic equation ($r > 0.92$).

DNA Content and Western Analysis of Cells from Discrete Spheroid Regions. In the previous experiments, all of the DNA-content and Western analyses were performed on mixtures of cells derived from all locations within the spheroid. To investigate the spatial distribution of cell proliferation and CKI expression within spheroids, we grew spheroids to ~1200 μm in diameter containing $\sim 1 \times 10^5$ cells. These spheroids were then selectively dissociated to yield cell suspensions from four discrete regions within the spheroid viable cell rim, with each fraction representing ~25% of the total spheroid cell number (33).[1] As documented previously (32, 35), Fig. 5 shows that there is a progressive decrease in cells with an S-phase DNA content with increasing depth in the spheroid, mirrored by an increase in the G_1-phase fraction. The G_2-phase DNA content fraction remained relatively constant at 10–15% for EMT-6 cells, and decreased from 15% to 4% in MEL28 cells. Western analysis of the same fractions (Figs. 6 and 7) indicated that $p18^{INK4c}$ and $p27^{Kip1}$ increased with increasing depth into the spheroid. The increase in $p18^{INK4c}$ (3–4-fold maximum) was higher than that of $p27^{Kip1}$ (2-fold

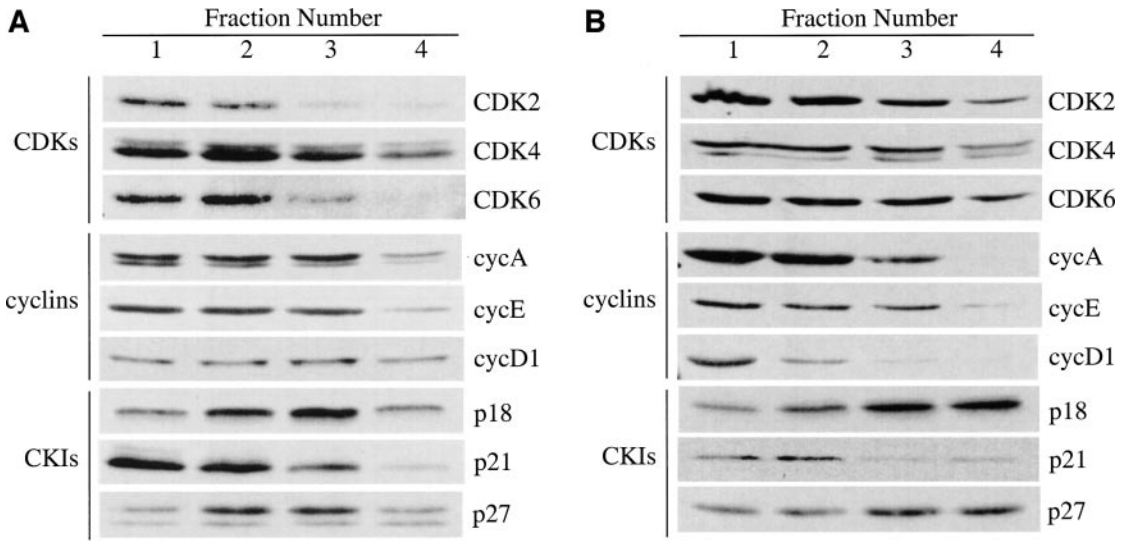

Fig. 6. Western analysis of G_1-phase regulatory protein expression in cells isolated from different locations within EMT6 (*A*) and MEL28 (*B*) spheroids of ~1200 um in diameter. *Fraction numbers*, cells from increasing depth within the spheroid and correspond to the four fractions shown in Fig. 7. Gels are representative of results from three to five independent experiments. *cyc*, cyclin; *CDK*, cyclin-dependent kinase; *CKI*, CDK inhibitor.

maximum) for both cell lines. The increase in $p18^{INK4c}$ and $p27^{Kip1}$ was detectable by the second fraction, which consists of cells only 30–60 μm from the spheroid surface. In both cell lines, $p18^{INK4c}$ and $p27^{Kip1}$ decreased in the cells from the innermost fraction to levels near that found in the outermost cells. Conversely, we noted a progressive decrease in the expression of $p21^{waf1/cip1}$, again detectable by the second fraction. In this case, there was essentially no detectable $p21^{waf1/cip1}$ in the innermost fraction.

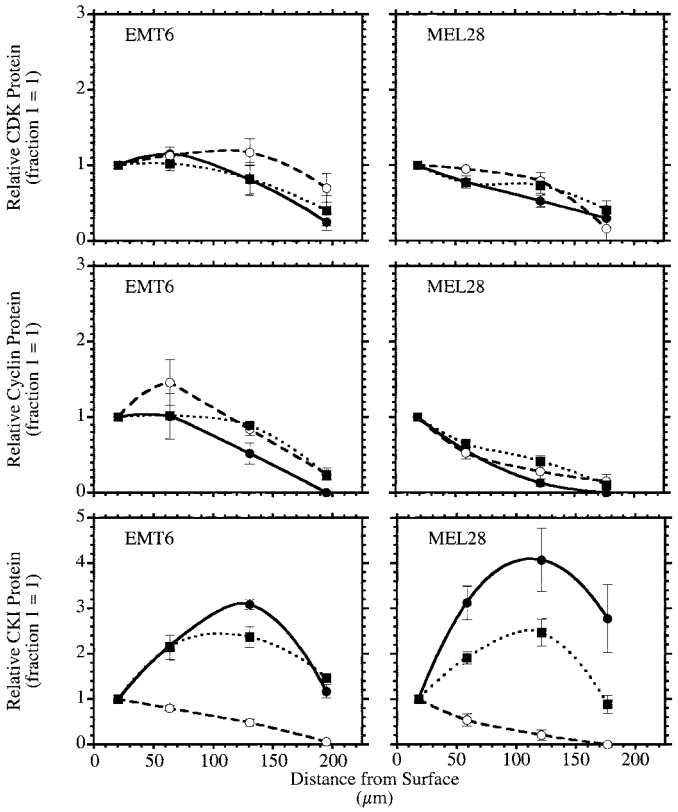

Fig. 7. Amounts of cyclin-dependent kinase inhibitors (*top panels*), cyclin dependent kinases (*middle panels*) and cyclins (*bottom panels*) as a function of location within EMT6 (*left*) and MEL28 (*right*) spheroids. CDK expression is shown for CDK2 (●, solid line), CDK4 (○, dashed line) and CDK6 (■, dotted line). Cyclin expression is shown for cyclin D1 (●, solid line), cyclin A (○, dashed line) and cyclin E (■, dotted line). CKI expression is shown for p18 (●, solid line), p21 (○, dashed line), and p27 (■, dotted line). Values are expressed relative to the amount of protein detected in the outermost fraction on each individual gel and represent means ± SEs for three to six separate experiments; *lines*, interpolations to the data. *CDK*, cyclin-dependent kinase; *CKI*, CDK inhibitor.

One trivial explanation for the changes observed in Figs. 6 and 7 would be that the dissociation procedure itself altered protein expression in the cells. This seems unlikely because the entire procedure required only 30–35 min, and the levels of different proteins increased, decreased, or stayed the same in different cell fractions. However, we did conduct several control experiments to investigate the effect of the dissociation on protein expression. Exponentially growing and plateau-phase monolayers were exposed to the trypsin dissociation buffer for up to 1 h at 37°C with no detectable alteration in the levels of $p18^{INK4c}$, $p21^{waf1/cip1}$, or $p27^{Kip1}$ (data not shown). In a separate experiment, we dissociated spheroids into four fractions as above and then replated the cells in monolayer culture. For the cells from the innermost region, we did observe a decrease in the levels of $p18^{INK4c}$ and $p27^{Kip1}$ and an increase in $p21^{waf1/cip1}$, but only after 4 h in monolayer culture (data not shown). In a third experiment, we dissociated a population of spheroids as described and then combined all of the cells together in one sample. A second set of spheroids was frozen intact with no dissociation. Western analysis of proteins extracted from these two samples showed no detectable difference in any of the proteins shown in Figs. 6 and 7. Finally, we have done some limited immunohistochemistry analysis of frozen sections of spheroids that show patterns of $p18^{INK4c}$, $p21^{waf1/cip1}$, and $p27^{Kip1}$ expression *in situ* (Fig. 8). We chose to perform immunohistochemistry of these three CKIs because they showed the most dramatic alteration in the Western results. The images in Fig. 8 clearly demonstrate that $p21^{waf1/cip1}$ is expressed primarily on the outside of the spheroid, and both $p18^{INK4c}$ and $p27^{Kip1}$ are expressed primarily in the middle and inner spheroid regions, very similar to the pattern of expression shown in Figs. 6 and 7. Thus, although the dissociation procedure may slightly alter protein expression levels, it seems extremely unlikely that the results shown in Figs. 6 and 7 are due to the dissociation procedure as opposed to representing the status of the cells in the spheroid.

To further clarify the role of CKIs in regulating cell cycle progression in different regions of spheroids, we also performed Western analysis of cyclins and CDKs associated with the G_1-phase and the

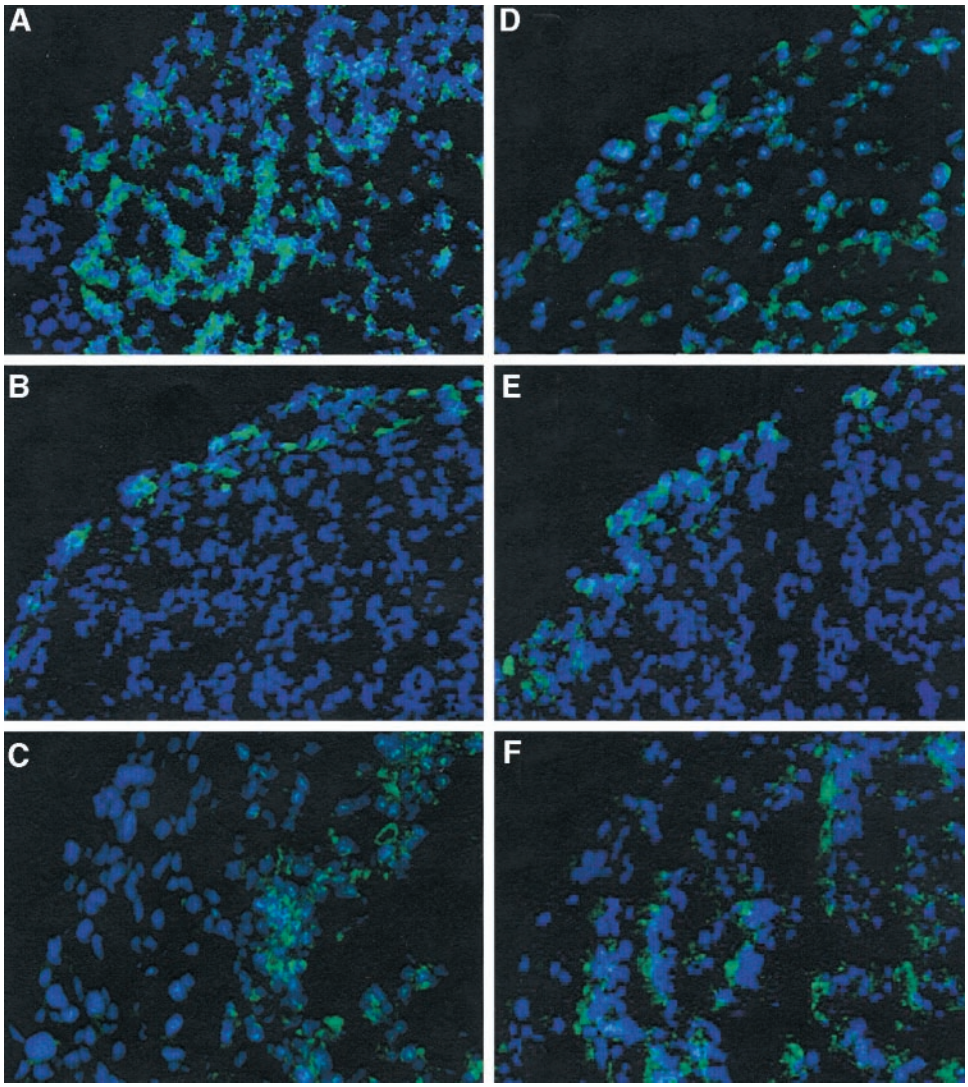

Fig. 8. Immunohistochemistry of cyclin-dependent kinase inhibitors (CKIs) in sections of EMT6 (*A–C*) and MEL28 (*D–F*) spheroids. Nuclei (*blue*) are counterstained with the DNA-binding dye DAPI and protein expression (*green*) is identified by fluorescently labeled antibody staining as described in the "Materials and Methods." Shown are representative images from antibody staining directed against p18 (*A* and *D*), p21 (*B* and *E*), and p27 (*C* and *F*). All of the images are oriented as follows: *the top left-hand corner,* the outer edge of the spheroid; *the bottom right-hand corner,* the beginning of the spheroid necrotic center.

G_1- to S-phase transition (Figs. 6 and 7). In general, there was a relatively constant expression of CDKs 2, 4, and 6 in the first three fractions, with a decrease in the innermost fraction. The level of CDK2 in MEL28 spheroids appeared to decrease progressively with increasing depth in the spheroid. Except for the case of CDK4 in EMT6 spheroids, the levels of all of the G_1-phase CDKs in the innermost fraction were less than one-half that found in the outer, proliferating cells. The levels of cyclins D1 and A were relatively constant in the outer fractions of EMT6 spheroids but decreased in the inner fractions. There was a progressive decrease in cyclins D1, A, and E in MEL28 spheroids. In both cell lines, the levels of the cyclins involved in G_1- to S-phase transition were essentially undetectable in the innermost fraction. It is interesting to note that expression of all proteins, including $p18^{INK4c}$ and $p27^{Kip1}$, was decreased in the innermost cell fraction of spheroids of both cell lines. The innermost fraction of MEL28 spheroids had a low expression of all CDKs and cyclins measured, but expression of $p18^{INK4c}$ remained elevated relative to the outermost fraction.

Cell Proliferation in Discrete Regions of EMT6 Spheroids. One ambiguity with conventional flow cytometric DNA content analysis is that knowledge of position in the cell cycle does not equate to proliferative status, because cells can be arrested in any stage of the cell cycle (36, 37). To obtain an accurate estimate of the proliferative status of cells in spheroids, we used simultaneous cytometric measurement of DNA content and BrdUrd incorporation to compare the percentage of cells in S phase to those actively replicating their DNA. Spheroids measuring ~1200 μm in diameter were given a 30-min pulse label of BrdUrd and then were dissociated into four equal fractions, and the results of this analysis were compared with standard DNA content analysis. As shown in Fig. 9, the percentage of EMT6 cells found to be actually incorporating BrdUrd decreased from 43% to 3% with increasing depth into the spheroid viable rim, whereas the percentage of cells with S-phase DNA content decreased only from 39% to 12%. In MEL28 spheroids, there was a much closer concordance between the DNA content data and BrdUrd incorporation assay. The percentage of MEL28 cells found to be actually incorporating BrdUrd decreased from 50% to 2% with increasing depth into the spheroid, whereas the percentage of cells with S-phase DNA content decreased from 47% to 4%. These results indicated that conventional DNA content analysis can lead to an underestimation of the number of nonproliferating cells. Although outer-region S-phase cells were actively synthesizing DNA in both cell lines, many inner-region EMT6 cells with an S-phase DNA content were not progressing through the cell cycle. There was also an indication of a G_2-phase arrest in the EMT6 cells, because the G_2-phase fraction remained essentially constant (15- 18%) whereas the percentage of cells incorporating BrdUrd was decreasing.

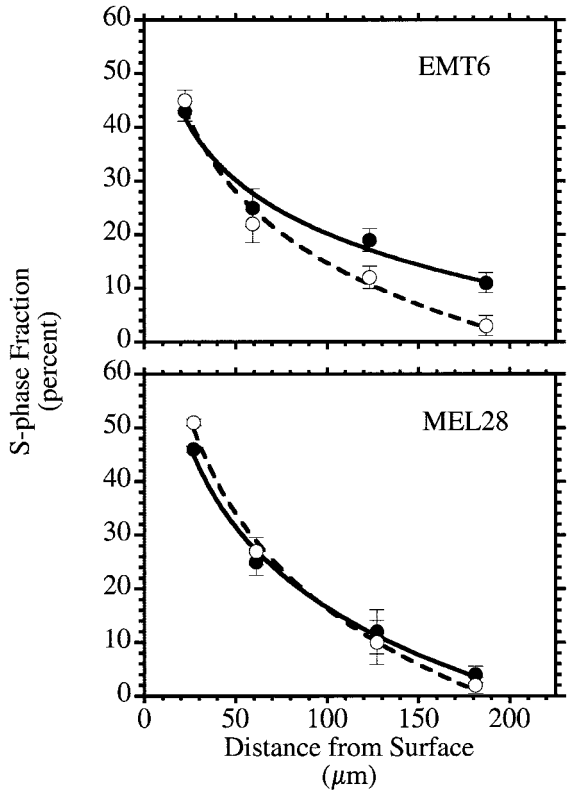

Fig. 9. Fraction of EMT6 (*top panel*) and MEL28 (*bottom panel*) cells with S-phase DNA content (●, solid line) compared with percentage of cells incorporating BrdUrd into their DNA (○, dashed line) as a function of location within the spheroid. *Data points* and *error bars* are as described in Fig. 2 ($n = 3$); *lines*, least-squares best fits to a logarithmic equation ($r > 0.98$).

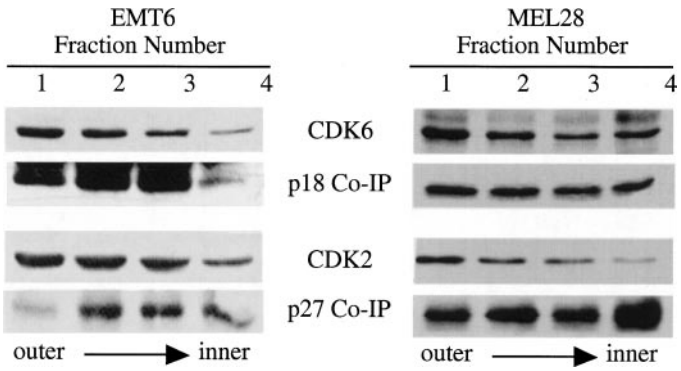

Fig. 10. Coimmunoprecipitation (*Co-IP*) analysis of CDK inhibitor (CKI) and cyclin-dependent kinase (*CDK*) association in cells isolated from different locations within EMT6 (*left panel*) and MEL28 (*right panel*) spheroids ~1200 μm in diameter. To demonstrate CDK/CKI interaction, cell lysates were immunoprecipitated with antibodies to CDK2 or CDK6, and the immunoprecipitates were analyzed by SDS-PAGE and Western analysis with antibodies to the CDK and the associated CKIs. *Fraction numbers*, cells from increasing depth within the spheroid and correspond approximately to the four fractions shown in Fig. 7.

Immunoprecipitation and Activity Analysis of CKI-CDK Complex Formation. Expression of CKIs is not in itself sufficient to inhibit CDK function; the CKIs must associate, in the appropriate ratio, with their target CDK to block CDK phosphorylation and activation by upstream regulatory proteins (9–11). The data in Fig. 7 suggested that not only were $p18^{INK4c}$ and $p27^{Kip1}$ elevated in the spheroid regions in which cell cycle arrest begins, but the levels of their target CDKs were also reduced. For example, in MEL28 spheroids, the ratio of $p27^{Kip1}$:CDK2 in fraction 3 was 3.8 times higher than in fraction 1, and the ratio of $p18^{INK4c}$:CDK6 was 5.6 times higher. To investigate this relationship more directly, coupled immunoprecipitation-Western blotting experiments were carried out to study the association of the CKIs with G_1- and G_1-S-phase CDK proteins, and to determine whether the association changed in accordance with alterations in cell cycle distribution in distinct regions of the spheroid (Fig. 10). In both cell types, we found that, although the overall levels of CDK2 decreased with increasing depth into the spheroid, the amount of $p27^{Kip1}$ found complexed to this protein increased. Similarly, in both cell types, the overall level of CDK6 decreased in the inner spheroid region, but the relative amount of coimmunoprecipitated $p18^{INK4c}$ increased. These observations suggested that both early and late G_1-phase CDK-mediated events were progressively inhibited in the interior regions of EMT6 spheroids, accounting for the accumulation of noncycling cells.

To address whether CDK activity was in fact being inhibited by the increased association of CKIs in the inner spheroid regions of the EMT6 and MEL28 spheroids, we performed coupled immunoprecipitation and kinase activity assays on cyclin/CDK6 and cyclin/CDK2 complexes isolated from the four regions of the spheroids. We were unable to demonstrate CDK6 activity under any *in vitro* conditions in either cell type, suggesting that this kinase has very weak activity, that our conditions were not optimized, or a combination of the two. This former possibility is reasonable because most published accounts of CDK6 activity use cells designed to overexpress the kinase or *in vitro* reconstitutions with high concentrations of complex components (14). However, when we examined CDK2 activity, with purified Histone H1 protein as substrate, we found that kinase activity did decrease at increasing depth into the spheroid (Fig. 11). In EMT6 cell extracts, the level of CDK2 activity appeared to correlate more strongly with its level of expression, rather than associated $p27^{Kip1}$, whereas in MEL28 cell extracts, Histone H1 phosphorylation was almost completely abrogated by the second fraction, indicating very efficient inhibition of activity.

DISCUSSION

Multicellular spheroids are known to mimic the growth characteristics of tumors and to develop gradients in proliferation with increasing size (1–3). The quiescent state is generally assumed to be a response to microenvironmental stresses, such as nutrient or growth factor gradients, which develop within the cell aggregates. Although many of the metabolic and physiological adaptations accompanying quiescence in spheroids are known (6, 31, 32, 36, 38, 39), neither the inducing signal(s) nor the ensuing molecular responses are understood. In both EMT6 and MEL28 spheroids, we found differential expression of $p18^{INK4c}$, $p21^{waf1/cip1}$, and $p27^{Kip1}$ with respect to their location in the spheroid. $p21^{waf1/cip1}$ was expressed in the outer, proliferating cells, whereas $p18^{INK4c}$ and $p27^{Kip1}$ expression became elevated with increasing depth into the spheroid, in concordance with

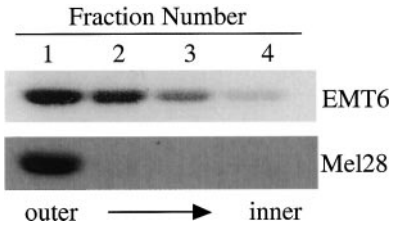

Fig. 11. Kinase assay analysis of cyclin-dependent kinase (CDK)2 activity in cells isolated from different locations within EMT6 (*top panel*) and MEL28 (*bottom panel*) spheroids of ~1200 μm in diameter. Cell lysates were immunoprecipitated with antibodies to CDK2, and the immunoprecipitated complexes were assayed for kinase activity against purified Histone H1 protein. *Fraction numbers*, cells from increasing depth within the spheroid; they correspond to the four fractions shown in Fig. 7.

proliferative arrest. Furthermore, in both cell types, we found a decrease in the expression of CDK2 and CDK6, and an increase in the relative amounts of $p27^{Kip1}$ and $p18^{INK4c}$ CKIs bound to these kinases. However, in EMT6 cells, CDK2 kinase activity decreased in proportion to its expression, whereas in MEL28 cells, CDK2 activity was completely inhibited by the second fraction, despite protein expression. There are several possible explanations for why the two cell lines differ in this respect. The EMT6 cell line is highly malignant and could contain a mutation in either $p27^{Kip1}$ or CDK2 that allows association of the two proteins but that does not permit the $p27^{Kip1}$-induced conformational change in CDK2 that inhibits its activity (40). Alternatively, although we did demonstrate an increase in $p27^{Kip1}$ association with CDK2, it is possible that unbound, active CDK2 remained in the cell.

The DNA content analyses presented in this study indicate that although the principle response of cells under these conditions is G_1-phase arrest, cells are also arrested in the S- and G_2-phases of the cell cycle. However, the EMT6 cells had a much higher ratio of nonproliferating:proliferating cells in S phase (S-phase arrest) than did the MEL28 cells, as well as more G_2-phase arrested cells. Given that the two cell lines differ with respect to both CDK2 kinase activity and in their ratio of G_1-phase to S- and G_2-phase arrested cells, we propose the following hypothesis. In the inner three fractions of MEL28 spheroids, both CDK6 and CDK2 activity is inhibited, resulting in an almost complete accumulation of cells in G_1. Conversely, in the EMT6 spheroids, any cell that has passed the CDK6-mediated checkpoint will then also pass through the deregulated CDK2/$p27^{Kip1}$ checkpoint and arrive in S phase. There, because of unknown factors, the cell will be unable to replicate its DNA and arrest, or will pass into G_2 phase and arrest. In both cell types, the S- and G_2-phase arrest may be due to specific alterations in S- and G_2-phase regulatory proteins, or may reflect the effect of a substance released from the spheroid necrotic center that nonspecifically induces arrest in all phases of the cell cycle (6, 41). S-phase arrest has been observed in cells from tumors, and is indicative of extreme physiological conditions (37, 42). Given that arrest can occur in all phases of the cell cycle, this study emphasizes the complexity of the system and the sensitivity with which cells respond to perturbations in their environment. Moreover, in light of the observation that in two different cell types, in two different species, we see microenvironmentally induced $p27^{Kip1}$ accumulation and association with CDK2, our data indicate that this pathway is an important and highly conserved response to the stresses encountered in the tumor environment.

The challenge remains to elucidate the signal(s) in the spheroid environment that regulates the expression of CKI proteins. $p21^{waf1/cip1}$ is induced by a variety of signals, including disruption of cell-matrix interactions (43), decreased pH (44), genotoxic stress (45, 46), hypoxia (47), and nitric oxide (48). Generally, and in direct contrast to what is observed in this study, these increases occur in conjunction with cell cycle delay (46, 49). The distribution of $p21^{waf1/cip1}$ to the proliferating regions of the spheroid precludes its involvement, as a CDK inhibitor, in maintaining cell cycle arrest in this model. However, the lack of $p21^{waf1/cip1}$ in nonproliferating cells may reflect the putative role of this protein in DNA synthesis, as a part of a CDK/Cyclin/$p21^{waf1/cip1}$/proliferating cell nuclear antigen (PCNA) complex (24, 50). The question remains as to why its expression increases in small, proliferating spheroids as compared with exponentially growing monolayer cells. One intriguing possibility that could reconcile this disparity is that, during initial aggregate culture, the primary role of $p21^{waf1/cip1}$ is not that of a CDK inhibitor, but rather that of an inhibitor of stress-activated protein kinase (SAPK/JUNK; Ref. 51). Conceivably, by inhibiting the activity of signal transduction pathways normally induced by "suboptimal" or stressful conditions, $p21^{waf1/cip1}$ could be enabling the cells to proliferate under conditions that would otherwise lead to apoptosis or arrest. A recent report by Mueller *et al.* (52) demonstrated that HCT116 colon carcinoma cells lacking $p21^{waf1/cip1}$ could no longer proliferate in aggregate cultures, supporting the above hypothesis.

The signals that induce $p27^{Kip1}$ expression have been well characterized. Its expression is modified by transforming growth factor β (TGF-β; Ref. 53), cAMP (54), serum deprivation (55), glucose concentration (56), anchorage-independent growth (57), and cell–cell contact (53). Control of protein expression has been reported to be primarily posttranscriptional (58), occurring at the level of mRNA stability (59), translational efficiency (54), and, most commonly, protein decay (58, 60). A recent article (61) reported that $p27^{Kip1}$ was uniformly up-regulated in small aggregate cultures of EMT6 cells, as opposed to the spatially specific distribution described here. However, close attention to the methods used in the spheroid culture strongly suggests that all of the cells in the cultures were severely nutrient deprived, and it may be that $p27^{Kip1}$ was induced by a stressful environment, as we report, and not by aggregate culture *per se*. These authors also show that treatment of the spheroids with collagenase decreases $p27^{Kip1}$ expression, but this could also be because of the alterations in the spheroid environment, including medium resupply and expansion of the extracellular space, allowing more efficient nutrient penetration into the spheroid. We have preliminary data showing that removal of cells from the spheroid microenvironment causes a very rapid (<4-h) disappearance of $p27^{Kip1}$, supporting this alternative interpretation.

The physiological stimuli that induce $p18^{INK4c}$ have not been well defined. However, there is evidence, with the closely related $p16^{INK4a}$ and $p15^{INK4b}$ proteins, that INK4-CKI association with CDK4 occurs at the expense of $p27^{Kip1}$, which then binds and inhibits CDK2 (62, 63). In both cell types, we saw an increase in the ratio of $p18^{INK4c}$ bound to CDK6 and $p27^{Kip1}$ bound to CDK2, suggesting that this may be occurring in spheroids. The observations that both of these CKIs are induced by the spheroid microenvironment, combined with their interaction with two different G_1-phase CDKs, strongly suggests that G_1-phase arrest is a highly conserved response to microenvironmental stress. The fact that EMT6 cells show a poor response in the $p27^{Kip1}$/CDK2 pathway, yet still arrest mostly in G_1-phase demonstrates the redundancy in cell cycle control.

Although we have begun to characterize the molecular changes that accompany cell cycle arrest in the multicellular spheroid, the physiological signals that induce these changes remain unknown. In a spheroid 1200 μm in diameter, the viable rim of cells surrounding the necrotic core is ~225 μm thick (6, 33, 34), and, of that viable rim, only the outer two to three cell layers are proliferating at the rate of exponentially growing monolayer cultures. Given that detectable changes in DNA content and expression of cell cycle regulatory proteins are observed 60 μm from the spheroid surface, these results strongly suggest that the signals inducing the changes in CKI and CDK expression are activated by very small changes in the spheroid microenvironment or by microenvironmental alterations that occur close to the spheroid surface. Although it is generally believed that hypoxia is related to cellular quiescence in solid tumors, there is evidence from the multicellular spheroid model that proliferative arrest occurs at relatively high oxygen concentrations (31, 35, 63). Our data support these studies because: (*a*) we see an increase in CKI expression and G_1-phase fraction in spheroids consisting of as few as ~200 cells, a size at which oxygen should not be a limiting factor; and (*b*) there is significant induction of CKIs and a decrease in S-phase cells only 60 μm into the spheroid cell rim in large spheroids, a region that has been shown to have an oxygen tension many times higher than that which induces arrest in single-cell cultures (64). Further-

more, our unpublished results indicate that acute oxygen deprivation leads to arrest in all phases of the cell cycle, as opposed to the predominantly G_1-phase-specific arrest presented here. This is in accordance with a recent report showing that severe hypoxia induces cell cycle arrest through alterations in CDK2,[2] which has a significantly reduced expression in the hypoxic regions of spheroids. On the basis of our present data, it is likely that more than one microenvironmental signal is acting to induce proliferation arrest in spheroids. Alternative signals that are relevant for the tumor microenvironment include lactate, glutamine, and glucose concentrations and pH, as well as growth factors, hormones, growth inhibitors, and extracellular matrix interactions.

The present finding of a differential expression of CKIs as a function of location within the spheroid also has implications for understanding CKI expression patterns in tumors. Recent work from several laboratories has demonstrated that expression of CKIs is variable between different tumors, and there have been many reports suggesting that expression of $p27^{Kip1}$ correlates with tumor stage, metastatic potential, and prognosis in a wide range of tumors (65–83). Interestingly, unlike what is observed with other CKIs (84–88), specific mutations or deletions in the *$p27^{Kip1}$* gene account for decreased expression in less than 1% of the tumors analyzed (60, 89–91); the primary mechanisms found to date are enhanced protein degradation via the ubiquitin pathway (92), and gene methylation (93). Although the majority of reports indicate a strong correlation between $p27^{Kip1}$ expression and tumor malignancy, this is not a universal phenomenon (94), particularly with endocrine tumors (95). Most work with human tumors involves measuring expression of a particular CKI in an extract from a tumor sample or by immunohistochemical analysis of tumor sections with little or no consideration of microregional heterogeneity in expression. Thus, some degree of the variability in CKI expression observed in tumors is probably a result of microenvironmental heterogeneity, and global estimates of CKI expression may be misleading. Furthermore, our spheroid data show that induction of specific CKI expression by microenvironmental stress regulates tumor cell proliferation, implying that the loss or functional mutation of a specific CKI gene during malignant progression would lead to disruption of one of the few remaining mechanisms of proliferation control in tumors. This may explain the correlations observed between $p27^{Kip1}$ expression and prognosis, and suggests that an understanding of the role of CKIs in microregional proliferation control in tumors will have important therapeutic implications.

A final interesting result of these studies is the decrease in essentially all of the cell cycle regulatory proteins observed in the innermost spheroid fraction. As shown in Fig. 7, these viable but nonproliferating cells have very low levels of cyclins D1, A, and E, reduced CDKs 2, 4, and 6, and essentially no $p21^{waf1/cip1}$. Even the two CKIs that were induced in the middle spheroid region decrease in the innermost fraction. Experiments in which spheroids were dissociated into 10 fractions of cells showed that the innermost 10% of the population had essentially no expression of any of these cell cycle regulatory proteins.[1] It is important to note that there were no changes in either CDK or cyclin expression in small spheroids despite increases in CKI expression that accompanied the progressive accumulation of nonproliferating cells (Figs. 3 and 4). The down-regulation of CDKs, cyclins, $p27^{Kip1}$, and $p18^{INK4c}$ was only seen in the innermost cells of large spheroids near the necrotic core, suggesting that this type of protein regulation is related to microenvironmental stress. As has been demonstrated previously (35), these innermost cells of both of these cell lines can re-enter the cell cycle when removed from the spheroid microenvironment, but they show a very long lag period before resuming proliferation. We have shown that the loss of mitochondrial function and its subsequent recovery after replating is correlated with cell cycle arrest and resumption of proliferation (38). The present results also suggest that the lag in proliferation for quiescent cells may be due, in part, to the need for these microenvironmentally stressed cells to basically reconstruct their entire cell cycle regulatory machinery. Preliminary work has shown that regrowth of these cells is preceded by marked increases in the levels of CDKs 2 and 6, cyclin D1, and $p21^{waf1/cip1}$. Thus, it appears that tumor cell cycle regulation by the microenvironment is a complex interaction of CKI induction and stress-induced regulatory protein degradation.

[2] S. L. Green and A. J. Giaccia. CDK2 activity is down-regulated by Thr14/Tyr15 phosphorylation under hypoxia, submitted for publication.

ACKNOWLEDGMENTS

We acknowledge Dan Shen and Vijaya Doddi for technical assistance with culturing and assaying the spheroids, and Robert Habbersett for assistance with the flow cytometric BrdUrd incorporation assays. We also acknowledge Dr. Albert van der Kogel and Hans Peters of the Department of Radiation Oncology, University Medical Center, Nijmegen, the Netherlands, for preparation of the immunohistochemistry sections of spheroids.

REFERENCES

1. Sutherland, R. M. Cell and environment interactions in tumor microregions: the multicell spheroid model. Science (Wash. DC), *240:* 177–184, 1988.
2. Freyer, J. P. Spheroids in radiobiology research. *In*: R. Bjerkvig (ed.), Spheroid Culture in Cancer Research, pp. 217–275. Boca Raton: CRC Press, 1992.
3. Mueller-Klieser, W. 3-dimensional cell cultures: from molecular mechanisms to clinical applications. Am. J. Physiol. Cell. Physiol., *42:* C1109–C1123, 1997.
4. Brown, J. M., and Giaccia, A. J. The unique physiology of solid tumors: opportunities (and problems) for cancer therapy. Cancer Res., *58:* 1408–1416, 1998.
5. Vaupel, P. W. The influence of tumor blood flow and microenvironmental factors on the efficacy of radiation, drugs and localized hyperthermia. Klin. Padiatr., *209:* 243–249, 1997.
6. Freyer, J. P. Role of necrosis in regulating the growth saturation of multicellular spheroids. Cancer Res., *48:* 2432–2439, 1988.
7. Marusic, M., Bajzer, Z., Vuk-Pavlovic, S., and Freyer, J. P. Tumor growth *in vivo* and as multicellular spheroids compared by mathematical models. Bull. Math. Biol., *56:* 617–631, 1994.
8. Sutherland, R. M., Ausserer, W. A., Murphy, B. J., and Laderoute, K. R. Tumor hypoxia and heterogeneity: challenges and opportunities for the future. Semin. Radiat. Oncol., *6:* 59–70, 1996.
9. Hunter, T., and Pines, J. Cyclins and cancer II: cyclin D and CDK inhibitors come of age. Cell, *79:* 573–582, 1994.
10. Sherr, C. J., and Roberts, J. M. Inhibitors of mammalian G1 cyclin-dependent kinases. Genes Dev., *9:* 1149–1163, 1995.
11. Morgan, D. O. Principles of CDK regulation. Nature (Lond.), *374:* 131–134, 1995.
12. Pines, J. Cyclin-dependent kinase inhibitors: the age of crystals. Biochim. Biophys. Acta, *1332:* M39–M42, 1997.
13. Hirai, H., Roussel, M. F., Kato, J-Y., Ashmun, R. A., and Sherr, C. J. Novel INK4 proteins, p19 and p18, are specific inhibitors of the cyclin D-dependent kinases CDK4 and CDK6. Mol. Cell. Biol., *15:* 2672–2681, 1995.
14. Guan, K-L., Jenkins, C. W., Li, Y., Nichols, M. A., Wu, X., O'Keefe, C. L., Matera, A. G., and Xiong, Y. Growth suppression by p18, a $p16^{INK4/MST1}$- and $p14^{INK4B/MST2}$-related CDK6 inhibitor, correlates with wild-type pRb function. Genes Dev., *8:* 2939–2952, 1994.
15. Weinberg, R. A. The retinoblastoma protein and cell cycle control. Cell, *81:* 323–330, 1995.
16. Lois, A. F., Cooper, L. T., Geng, Y., Nobori, T., and Carson, D. Expression of the p16 and p15 cyclin-dependent kinase inhibitors in lymphocyte activation and neuronal differentiation. Cancer Res., *55:* 4010–4013, 1995.
17. Franklin, D. S., and Xiong, Y. Induction of $p18^{INK4c}$ and its predominant association with CDK4 and CDK6 during myogenic differentiation. Mol. Biol. Cell, *7:* 1587–1599, 1996.
18. Alcorta, D. A., Xiong, Y., Phelps, D., Hannon, G., Beach, D., and Barrett, J. C. Involvement of the cyclin-dependent kinase inhibitor p16(INK4a) in replicative senescence of normal human fibroblasts. Proc. Natl. Acad. Sci. USA, *93:* 13742–13747, 1996.
19. Reed, A. L., Califano, J., Cairns, P., Westra, W. H., Jones, R. M., Koch, W., Ahrendt, S., Eby, Y., Sewell, D., Nawroz, H., Bartek, J., and Sidransky, D. High frequency of p16CDKN2/MTS-1/INK4a inactivation in head and neck squamous carcinoma. Cancer Res., *56:* 3630–3633, 1996.
20. Kim, J. R., Kim, S. Y., Kim, M. J., and Kim, J. H. Alterations of CDKN2 (*MTS1/$p16^{INK4A}$*) gene in paraffin-embedded tumor tissues of human stomach, lung, cervix and liver cancers. Exp. Mol. Med, *30:* 109–114, 1998.

21. Waldman, T., Kinzler, K. W., and Vogelstein, B. p21 is necessary for the p53-mediated G_1 arrest in human cancer cells. Cancer Res., *55:* 5187–5190, 1995.
22. Toyoshima, H., and Hunter, T. p27, a novel inhibitor of G1 cyclin-Cdk protein kinase activity, is related to p21. Cell, *75:* 67–74, 1994.
23. LaBaer, J., Garrett, M. D., Stevenson, L. F., Slingerland, J. M., Sandhu, C., Chou, H. S., Fattaey, A., and Harlow E. New functional activities for the p21 family of CDK inhibitors. Genes Dev., *11:* 847–862, 1997.
24. Zhang, H., Hannon, G. J and Beach, D. p21-containing cyclin kinases exist in both active and inactive states. Genes Dev., *8:* 1750–1758, 1994.
25. LaRue, K. E., Bradbury, M. E., and Freyer, J. P. Regulation of G1 transit by cyclin kinase inhibitors in multicellular spheroid cultures of rat embryo fibroblast cells transformed to different extents. Cancer Res., *58:* 1305–1314, 1998.
26. Kerbel, R. S., Rak, J., Kobayashi, H., Man, M. S., St. Croix, B., and Graham, C. H. Multicellular resistance: a new paradigm to explain aspects of acquired drug-resistance of solid tumors. Cold Spring Harbor Symp. Quant. Biol., *59:* 661–672, 1994.
27. Ikebe, M., and Tiecher, B. A. Alterations in gene expression between EMT6 mammary carcinoma monolayers and spheroids identified by differential display. Int. J. Oncol., *9:* 629–634, 1996.
28. Phillips, R. M., and Clayton, M. R. K. Plateau-phase cultures: an experimental model for identifying drugs which are bioactive within the microenvironment of solid tumours. Br. J. Cancer, *75:* 196–201, 1997.
29. Rockwell, S. C., Kallman, R. F., and Fajardo, L. F. Characteristics of a serially transplanted mouse mammary tumor and its tissue culture adapted derivative. J. Natl. Cancer Inst. (Bethesda), *49:* 735–747, 1972.
30. Carey, T. E., Takahashi, T., Resnick, L. A., Oettgen, H. F., and Old, L. J. Cell surface antigens of human malignant melanoma: mixed hemadsorption assays for humoral immunity to cultured autologous melanoma cells. Proc. Natl. Acad. Sci. USA, *73:* 3278–3282, 1976.
31. Freyer, J. P., and Sutherland, R. M. Regulation of growth saturation and development of necrosis in EMT6/Ro multicellular spheroids by the glucose and oxygen supply. Cancer Res., *46:* 3504–3512, 1986.
32. Freyer, J. P. Rates of oxygen consumption for proliferating and quiescent cells isolated from multicellular tumor spheroids. Adv. Exp. Med. Biol., *345:* 335–342, 1994.
33. Freyer, J. P., and Schor, P. L. Automated selective dissociation of cells from different regions of multicellular spheroids. In Vitro Cell. Dev. Biol., *25:* 9–19, 1989.
34. Crissman, H. A., Steinkamp, J. A. A new method for rapid and sensitive selection of bromodeoxyuridine in DNA-replicating cells. Exp. Cell Res., *173:* 256–261, 1987.
35. Lal, A., Peters, H., St. Croix, B., Haroon, Z. A., Dewhirst, M. W., Strausberg, R. L., Kaanders, J. H., van der Kogel, A. J., and Riggins, G. J. Transcriptional response to hypoxia in human tumors. J. Natl. Cancer Inst. (Bethesda), *93:* 1337–1343, 2001.
36. Freyer, J. P., and Schor, P. L. Regrowth kinetics of cells from different regions of multicellular spheroids of four cell lines J. Cell Physiol., *138:* 384–392, 1989.
37. Stubbs, M. C., Strachan, G. D., and Hall, D. J. An early S phase checkpoint is regulated by the E2F1 transcription factor. Biochem. Biophys. Res. Commun., *258:* 77–80, 1999.
38. Freyer, J. P., Schor, P. L., Jarrett, K. A., Neeman, M., and Sillerud, L. O. Cellular energetics measured by phosphorous NMR spectroscopy are not correlated with chronic nutrient deficiency in multicellular tumor spheroids. Cancer Res., *51:* 3831–3837, 1991.
39. Freyer, J. P. Decreased mitochondrial function in quiescent cells isolated from multicellular tumor spheroids. J Cell. Physiol., *176:* 138–149, 1998.
40. Russo, A. A., Jeffrey, P. D., Patten, A. K., Massague, J., and Pavletich, N. P. Crystal structure of the $p27^{Kip1}$ cyclin-dependent kinase inhibitor bound to the cyclin A cdk2 complex. Nature (Lond.), *382:* 325–333, 1996.
41. Freyer, J. P., and Schor, P. L., and Saponara, A. G. Partial purification of a protein growth inhibitor from multicellular spheroids. Biochem. Biophys. Res. Comm., *152:* 463–368, 1988.
42. Zolzer, F., Stuben, G., Knuhmann, K., Streffer, C., and Sack, H. Quiescent S-phase cells as indicators of extreme physiological conditions in human tumor xenografts. Int. J. Radiat. Oncol. Biol. Phys., *45:* 1019–1024, 1999.
43. Wu, R. C., and Schonthal, A. H. Activation of p53–$p21^{Waf1}$ pathway in response to disruption of cell-matrix interactions. J. Biol. Chem., *272:* 29091–29098, 1997.
44. Ohtsubo, T., Wang, X., Takahashi, A., Ohnishi, K., Saito, H., Song, C. W., and Ohnishi, T. p53-dependent induction of WAF1 by a low-pH culture condition in human glioblastoma cells. Cancer Res., *57:* 3910–3913, 1997.
45. El-Diery, W. S., Harper, J. W., O'Connor, P. M., Velculescu, V. E., Canman, C. E., Jackman, J., Peitenpol, J. A., Burrel, M., Hill, D. E., Wang, Y., Wiman, K. G., Mercer, W. E., Kastan, M. B., Kohn, K. W., Elledge, S. J., Kinzler, K. W., and Vogelstein, B. WAF1/CIP1 is induced in p53-mediated G_1 arrest and apoptosis. Cancer Res., *54:* 1169–1174, 1994.
46. Deng, C., Zhang, P., Harper, J. W., Elledge, S. J., and Leder, P. Mice lacking $p21^{Cip1/Waf1}$ undergo normal development, but are defective in G_1 checkpoint control. Cell, *82:* 675–684, 1995.
47. Graeber, T. G., Peterson, J. F., Tsai, M., Monica, K., Fornace, A. J., and Giaccia, A. J, Hypoxia induces accumulation of p53 protein, but activation of a G_1-phase checkpoint by low-oxygen conditions is independent of p53 status. Mol. Cell. Biol., *14:* 6264–6277, 1994.
48. Ishida, A., Sasaguri, T., Kosaka, C., Nojima, H., and Ogata, J. Induction of the cyclin-dependent kinase inhibitor $p21^{Sdi1/Cip1/Waf1}$ by nitric-oxide-generating vasodilator in vascular smooth muscle cells. J. Biol. Chem., *272:* 10050–10057, 1997.
49. Harper, J. W., Adami, G. R., Wei, N., Keyomarsi, K., and Elledge, S. J. The p21 CDK- interacting protein Cip1 is a potent inhibitor of G1 cyclin-dependent kinases. Cell, *75:* 805–816, 1993.
50. Cayrol, C., and Ducommun, B. Interaction of the cyclin-dependent kinase inhibitor p21 with PCNA: a link between cell cycle and DNA repair. Med. Sci., *13:* 1259–1265, 1997.
51. Shim, J., Lee, H., Park, J., Kim, H., and Choi, E. A non-enzymatic p21 protein inhibitor of stress-activated protein kinases. Nature (Lond.), *381:* 804–807, 1996.
52. Mueller, S., Cadenas, E., and Schonthal, A. H. $p21^{Waf1}$ regulates anchorage-independent growth of HCT116 colon carcinoma cells via E-cadherin expression. Cancer Res., *60:* 156–163, 2000.
53. Polyak, K., Kato, J-Y., Solomon, M. J., Sherr, C. J., Massague, J., Roberts, J. M., and Koff, A. p27Kip1, a cyclin-Cdk inhibitor, links transforming growth factor B and contact inhibition to cell cycle arrest. Genes Dev., *8:* 9–22, 1994.
54. Kato, J., Matsuoka, M., Polyak, K., Massague, J., and Sherr, C. J. Cyclic AMP-induced G_1 phase arrest mediated by an inhibitor ($p27^{Kip1}$) of cyclin-dependent kinase 4 activation. Cell, *79:* 487–496, 1994.
55. Coats, S., Flanagan, W. M., Nourse, J., and Roberts, J. M. Requirement of $p27^{Kip1}$ for restriction point control of the fibroblast cell cycle. Science (Wash. DC), *272:* 877–880, 1996.
56. Wolf, G., Schroeder, R., Ziyadeh, F. N., Thaiss, F., Zahner, G., and Stahl, R. A. K. High glucose stimulates expression of $p27^{Kip1}$ in cultured mouse mesangial cells: relationship to hypertrophy. Am. J Physiol. Renal Physiol., *42:* F348–F356, 1997.
57. Kawada, M., Uehara, Y., Mizuno, S., Yamori, T., and Tsuruo, T. Up-regulation of $p27^{Kip1}$ correlates inversely with anchorage-independent growth of human cancer cell lines. Jpn. J. Cancer Res., *89:* 110–115, 1998.
58. Pagano, M., Tam, S. W., Theodoras, A. M., Beer-Romero, P., Del Sal, G., Chau, V., Yew, P. R., Draetta, G. F., and Rolfe, M. Role of the ubiquitin-proteosome pathway in regulating abundance of the cyclin-dependent kinase inhibitor p27. Science (Wash. DC), *269:* 682–285, 1995.
59. Hengst, L., and Reed, S. I. Translational control of $p27^{Kip1}$ accumulation during the cell cycle. Science (Wash. DC), *271:* 1861–1864, 1996.
60. Kawada, M., Yamagoe, A., Murakami, Y., Suzuki, K., Mizuno, S., and Uehara, Y. Induction of $p27^{Kip1}$ degradation and anchorage independence by Ras through the MAP kinase signaling pathway. Oncogene, *15:* 629–637, 1997.
61. St. Croix, B., Florenes, V. A., Rak, J. W., Flanagan, M., Bhattacharya, N., Slingerland, J. M., and Kerbel, R. S. Impact of the cyclin-dependent kinase inhibitor $p27^{Kip1}$ on resistance of tumor cells to anticancer agents. Nat. Med., *11:* 1204–1210, 1996.
62. Reynisdottir, I., and Massague, J. The subcellular locations of $p15^{INK4b}$ and $p27^{Kip1}$ coordinate their inhibitory interactions with cdk4 and cdk2. Genes Dev., *11:* 492–505, 1997.
63. McConnel, B. B., Gregory, F. J., Stott, F. J., Hara, E., and Peters, G. Induced expression of p16(INK4a) inhibits both CDK4- and CDK2-associated kinase activity by reassortment of cyclin-CDK-inhibitor complexes. Mol. Cell. Biol., *19:* 1981–1989, 1999.
64. Mueller-Klieser, W., Freyer, J. P., and Sutherland, R. M. Influence of glucose and oxygen supply conditions on the oxygenation of multicellular spheroids. Br. J. Cancer, *53:* 345–353, 1986.
65. Lloyd, R. V., Erickson, L. A., Jin, L., Kulig, E., Qian, X., Cheville, J. C., and Scheithaur, B. W. $p27^{Kip1}$: a multifunctional cyclin-dependent kinase inhibitor with prognostic significance in human cancers. Am. J. Pathol., *150:* 313–323, 1999.
66. Anderson, J., Reddy, V. B., Green, L., Bitterman, P., Borok, R., Maggi-Galluzzi, C., Montironi, R., Wick, M., Gould, V. E., and Gattuso, P. Role of expression of cell cycle inhibitor p27 and MIB-1 in predicting lymph node metastasis in male breast carcinoma. Breast J., *8:* 101–107, 2002.
67. De Paola, F., Vecci, A. M., Granato, A. M., Liverani, M., Monti, F., Innoceta, A. M., Gianni, L., Saragoni, L., Ricci, M., Falcini, F., Amadori, D., and Volpi, A. p27/kip1 expression in normal epithelium, benign and neoplastic breast lesions. J. Pathol., *196:* 26–31, 2002.
68. Catzavelos, C., Bhattacharya, N., Ung, Y. C., Wilson, J. A., Roncari, L., Sandhu, C., Shaw, P., Yeger, H., Marava-Potzner, I., Kapuska, L., Franssen, E., Pritchard, K. I., and Slingerland, J. M. Decreased levels of the cell-cycle inhibitor p27Kip1 protein: prognostic implications in primary breast cancer. Nat, Med., *3:* 227–230, 1997.
69. Porter, P. L., Malone, K. E., Heagerty, P. J., Alexander, G. M., Gatti, L. A., Firpo, E. J., Daling, J. R., and Roberts, J. M. Expression of cell-cycle regulators p27Kip1 and cyclin E, alone and in combination, correlate with survival in young breast cancer patients. Nat. Med., *3:* 222–225, 1997.
70. Tan, P., Cady, B., Wanner, M., Worland, P., Cukor, B., Magi-Galluzzi, C., Lavin, P., Draetta, G., Pagano, M., and Loda, M. The cell cycle inhibitor p27 is and independent prognostic marker in small ($T_{1a,b}$) invasive breast carcinomas. Cancer Res., *57:* 1259–1263, 1997.
71. Loda, M., Cukor, B., Tam, S. W., Lavin, P., Fiorentino, M., Draetta, G. F., Jessup, J. M., and Pagano, M. Increased proteasome-dependent degradation of the cyclin-dependent kinase inhibitor p27 in aggressive colorectal carcinoma. Nat. Med., *3:* 231–234, 1997.
72. Sgambato, A., Ratto, C., Faraglia, B., Merico, M., Ardito, R., Schinzari, G., Romano, G., and Cittadini, A. R. Reduced expression and altered subcellular localization of the cyclin- dependent kinase inhibitor p27(Kip1) in human colon cancer. Mol. Carcinog., *26:* 172–179, 1999.
73. Singh, S. P., Lipman, J., Goldman, H., Ellis, F. H., Jr., Aizenman, L., Cangi, M. G., Signoretti, S., Chiaur, D. S., Pagano, M., and Loda, M. Loss or altered subcellular localization of p27 in Barrett's associated adenocarcinoma. Cancer Res., *58:* 1730–1735, 1998.
74. Migita, T., Oda, Y., and Naito, S., and Tsuneyoshi, M. Low expression of p27(Kip1) is associated with tumor size and poor prognosis in patients with renal cell carcinoma. Cancer (Phila.), *94:* 973–979, 2002.
75. Khoo, M. L., Beasley, N. J., Freeman, J. L., and Asa, S. L. Overexpression of cyclin D1 and underexpression of p27 predict lymph node metastases in papillary thyroid carcinomas. J. Clin. Endocrinol. Metab., *87:* 1814–1818, 2002.

76. Tshlias, J., Kapusta, L. R., DeBoer, G., Morava-Protzner, I., Zbieranowski, I., Bhattacharya, N., Catzavelos, G. C., Klotz, L. H., and Slingerland, J. M. Loss of cyclin dependent kinase inhibitor $p27^{Kip1}$ is a novel prognostic factor in localized human prostate adenocarcinoma. Cancer Res., *58:* 524–548, 1998.
77. Yang, R. M., Naitoh, H. J., Murphy, M., Wang, H-J., Phillipson, J., DeKernion, J. B., Loda, M., and Reiter, R. E. Low p27 expression predicts poor disease-free survival in patients with prostate cancer. J. Urol., *159:* 941–945, 1998.
78. Cheville, J. C., Lloyd, R. V., Sebo, T. J., Cheng, L., Erickson, L., Bostwick, D. G., Lohse, C. M., and Wollan, P. Expression of p27Kip1 in prostatic adenocarcinoma. Mod. Pathol., *11:* 324–328, 1998.
79. Del Pizzo, J. J., Borkowski, A., Jacobs, S. C., and Kyprianou, N. Loss of cell cycle regulators p27 (Kip1) and cyclin E in transitional cell carcinoma of the bladder correlates with tumor grade and patient survival. Am. J. Pathol., *155:* 1129–1136, 1999.
80. Sgambato, A., Migaldi, M., Faraglia, B., Garagnani, L., Romano, G., De Gaetani, C., Ferrari, P., Capelli, G., Trentini, G., and Cittadini, A. Loss of p27Kip1 expression correlates with tumor grade and with reduced disease-free survival in primary superficial bladder cancers. Cancer Res., *59:* 3245–3250, 1999.
81. Jordan, R. C., Bradley, G., and Slingerland, J. Reduced levels of the cell-cycle inhibitor p27Kip1 in epithelial dysplasia and carcinoma of the oral cavity. Am. J. Pathol., *152:* 585–590, 1998.
82. Florenes, V. A., Maelandsmo, G. M., Kerbel, R. S., Slingerland, J. M., Nesland, J. M., and Holm, R. Protein expression of the cell-cycle inhibitor p27Kip1 in malignant melanoma: inverse correlation with disease-free survival. Am. J. Pathol., *153:* 305–312, 1998.
83. Mouriaux, F., Casagrande, F., Pillaire, M. J., Manenti, S., Malecaze, F., Darbon, J. M. Differential expression of G1 cyclins and cyclin-dependent kinase inhibitors in normal and transformed melanocytes. Investig. Opthalmol. Vis. Sci., *39:* 876–884, 1998.
84. Burns, K. L., Ueki, K., Jhung, S. L., Koh, J., and Louis, D. N. Molecular-genetic correlates of p16, CDK4, and pRb immunohistochemistry in glioblastomas. J. Neuropathol. Exp. Neurol., *57:* 122–130, 1998.
85. Flores, J. F., Walker, G. J., Glendening, J. M., Haluska, F. G., Castresana, J. S., Rubio, M-P., Pastorfide, G. C., Boyer, L. A., Kao, W. H., Bulyk, M. L., Barnhill, R. L., Hayward, N. K., Housmann, D. E., and Fountain, J. W. Loss of $p16^{INK4a}$ and $p15^{INK4b}$ genes, as well as neighboring 9p21 markers, in sporadic melanoma. Cancer Res., *56:* 5023–5032, 1996.
86. Lapointe, J., Lachance, Y., Labrie, Y., and Labrie, C. A p18 mutant defective in CDK6 binding in human breast cancer cells. Cancer Res., *56:* 4586–4589, 1996.
87. Reed, A. L., Califano, J., Cairns, P., Westra, W. H., Jones, R. M., Koch, W., Arendt, S., Eby, Y., Sewell, D., Nawroz, H., Bartek, J., and Sidransky, D. High frequency of mutation of $p16^{CDKN2/MTS-1/INK4a}$ in head and neck squamous carcinomas. Cancer Res., *56:* 3630–3633, 1996.
88. Reymond, A., and Brent, R. p16 proteins from melanoma-prone families are deficient in binding to CDK4. Oncogene, *11:* 1173–1178, 1995.
89. Morosetti, R., Kawamata, N., Gombart, A. F., Miller, C. W., Hatta, Y., Hirama, T., Said, J. W., Tomonaga, M., and Koeffler, H. P. Alterations of the *p27Kip1* gene in non-Hodgkin's lymphomas and adult T-cell leukemia/lymphoma. Blood, *86:* 1924–1930, 1995.
90. Spirin, K. S., Simpson, J. F., Takeuchi, S., Kawamata, N., Miller, C. W., and Koeffler, H. P. p27Kip1 mutation found in breast cancer. Cancer Res., *56:* 2400–2404, 1996.
91. Tanaka, C.,. Yoshimoto, K., Yang, P., Kimura, T., Yamada, S., Moritani, M., Saro, T., and Itakura, M. Infrequent mutations of *p27Kip1* gene and trisomy 12 in a subset of human pituitary adenomas. J. Clin. Endocrinol. Metab., *82:* 3141–3147, 1997.
92. Morgan, M. B., and Cowper, S. E. Expression of p27 (kip1) in nevi and melanomas. Am. J. Dermatopathol., *21:* 121–124, 1999.
93. Qian, X., Jin, L., Kulig, E., and Lloyd, R. V. DNA methylation regulates p27Kip1 expression in rodent pituitary cell lines. Am. J. Pathol., *153:* 1475–1482, 1998.
94. Lloyd, R. V., Jin, L., Qian, X., and Kulig, E. Aberrant p27Kip1 expression in endocrine and other tumors. Am. J. Pathol., *150:* 401–407, 1997.
95. Canavese, G., Azzoni, C., Pizzi, S., Corleto, V. D., Pasquali, C., Dvoli, C., Crafa, P., Delle Fave, G., and Bordi, C. p27: a potential main inhibitor of cell proliferation in digestive endocrine tumors but not a marker of benign behavior. Hum. Pathol., *32:* 1094–1100, 2001.

Microenvironmental Regulation of Proliferation in Multicellular Spheroids Is Mediated through Differential Expression of Cyclin-Dependent Kinase Inhibitors

Karen E. A. LaRue, Mona Khalil and James P. Freyer

Cancer Res 2004;64:1621-1631.